Characteristics of boundary layer structure during a persistent haze-fog event in central Liaoning City Cluster, Northeast China

Journal:	*Journal of Meteorological Research (JMR)*
Manuscript ID	ACTA-E-2017-0053
Manuscript Type:	Special Issue on the Extremely Heavy Haze-Fog Episodes in Winter 2016 in the Beijing-Tianjin-Hebei Area of China
Date Submitted by the Author:	21-Apr-2017
Complete List of Authors:	Li, Xiaolan; Institute of Atmospheric Environment, CMA, ; Wang, Yangfeng; Institute of Atmospheric Environment, CMA Shen, Lidu; Shenyang Regional Climatic Center Zhang, Hongsheng; Department of Atmospheric and Oceanic Sciences, School of Physics, Peking University Zhao, Hujia; Institute of Atmospheric Environment, CMA Zhang, Yunhai; Institute of Atmospheric Environment, China Meteorological Administration Ma, Yanjun; Institute of Atmospheric Environment, CMA, ;
Keywords:	Haze-fog event, Thermal inversion layer, Atmospheric boundary layer, Northeast China
Speciality:	Atmospheric physics, Atmospheric boundary layer, Atmospheric environment

Characteristics of boundary layer structure during a persistent haze-fog event in central Liaoning City Cluster, Northeast China

LI Xiaolan[1] (李晓岚), WANG Yangfeng[1] (王扬锋), SHEN Lidu[2] (沈历都), ZHANG Hongsheng[3] (张宏升), ZHAO Hujia[1] (赵胡笳), ZHANG Yunhai[1] (张云海), MA Yanjun[1*] (马雁军)

1 *Institute of Atmospheric Environment, China Meteorological Administration, Shenyang* 110166

2 *Shenyang Regional Climatic Center, Shenyang 110166*

3 *Laboratory for Climate and Ocean-Atmosphere Studies, Department of Atmospheric and Oceanic Sciences, School of Physics, Peking University, Beijing 100871*

(Submitted April 21, 2017)

Supported by the Science and Technology Research Project (Doctoral Research Special Fund) of Liaoning Meteorological Office (D201603), National Key Project of MOST (2016YFC0203300), the National Natural Science Foundation of China (41605081), R&D Special Fund for Public Welfare Industry (meteorology) by Ministry of Finance and Ministry of Science and Technology (GYHY201406031), Basic Research Funds of Central Public Welfare Research Institutes (2016SYIAEZD3), and the CMA Special Funds of Core Business Development (CMAHX20160306).

*Corresponding author: mayanjun0917@163.com. Tel: 024-83893488; 13840072906

ABSTRACT

The characteristics of boundary layer structure during a persistent regional haze-fog event over the central Liaoning City Cluster of Northeast China during 16–21 December 2016 were investigated based on measurements of particulate matter (PM) concentrations and boundary layer data. The haze-fog event occurred firstly in Shenyang, followed by Fushun, Benxi, and Anshan, and PM concentrations were relatively higher in Anshan and Shenyang but lower in Benxi and Fushun. The daily mean horizontal vector wind fields during 16–21 December, calculated using the European Centre for Medium Range Weather Forecasts (ECMWF) Re-Analysis interim (ERA-Interim) data, indicated that a southerly flow prevailed during the early period of the haze-fog event, bringing water vapor from the Bohai Sea to the study region. During the haze-fog developing period, wind speed decreased rapidly, and a belt of low wind speed formed along the Anshan–Benxi line on 20 December. In terms of the vertical boundary layer structure, a weak thermal inversion layer existed at ground level at the beginning of the haze-fog event, which was overlain by a strong inversion layer in the near-surface layer. The bottom of this strong inversion layer was lifted from 200 to 900 m by a cold air mass, leading to strong vertical dispersion of pollutants and a decrease in the PM concentration at the surface. The stable atmospheric stratification finally acted on the vertical distribution of the wind field in the boundary layer and further weakened the exchange capacity of vertical turbulence. A stable wind direction, low wind speed, low boundary layer height (<600 m), and strong thermal inversion layer contributed to the formation and

development of this haze-fog event. A backward trajectory analysis revealed the different sources of air masses in the four cities and explained the different characteristics of the haze-fog episodes in the four cities.

Key words: Haze-fog event, Thermal inversion layer, Atmospheric boundary layer, Northeast China

1. Introduction

Fog and haze are meteorological phenomena that may lead to severe near-surface weather (Zhang et al., 2014). Haze-fog pollution in China has increased over the past three decades, particularly in city clusters, as a result of the rapidly developing economy, expansion of anthropogenic activities and urbanization (Shao et al., 2006; Fu et al., 2014; Wang et al., 2014a). In recent years, heavy and persistent haze-fog events have been observed in different regions of China (Ji et al., 2012; Liu et al., 2015; Peng et al., 2016), resulting in atmospheric visibility reduction, increased air pollution, and risks to public health (Chan and Yao, 2008; Che et al., 2014; Chen et al., 2012; Shen et al., 2015; Zhang et al., 2014; Tang et al., 2017).

Haze-fog formation is closely related to meteorological conditions and high aerosol mass loadings (Wang et al., 2014b). Therefore, severe haze-fog events commonly occur in the heating season and during periods when agricultural residues are burned, due to the large pollution emissions and unfavorable meteorological conditions for pollution dispersion (Fu et al., 2014; Wang et al., 2014b; Zheng et al., 2015; Chen et al., 2016). Because the heating season begins earlier and lasts longer in Northeast China than in most other regions in China and is combined with burning of agricultural residues that are largely concentrated in the early heating season, haze-fog events occur frequently during winter in this region. For example, a heavy and persistent haze-fog event with a maximum $PM_{2.5}$ concentration exceeding 1000 μg m^{-3} occurred during 1–8 November 2015 in Shenyang and profoundly shocked both the public and the government (http://news.sina.com.cn/c/nd/2015-11-08/doc-ifxknutf1607479.shtml). Several studies have reported that haze-fog pollution in Northeast China is serious (Cui et al., 2015), with an increasing trend in particulate matter (PM) observed at some stations in this region from 2006 to 2014 (Wang et al., 2015c).

Many efforts have been made to identify the meteorological causes of haze-fog events involving the effects of surface meteorological conditions, synoptic systems, climatic background, and local atmospheric circulation induced by the topography (Chen et al., 2008; Liu et al., 2009; Zhu et al., 2012). Chen et al. (2008) indicated that pollution formation is related to high-pressure conditions and successive low-pressure systems over North China. Zhu et al. (2012) demonstrated that the weakened monsoon circulation of recent decades has made a significant contribution to trapping pollutants over Eastern China. The modeling results reported by Miao et al. (2015) revealed that local atmospheric circulation plays an important role in surface air pollution over the Beijing–Tianjin–Hebei region. In addition, the structure of the atmospheric boundary layer (ABL) is also crucial to the formation and evolution of haze-fog (Wang et al., 2006; Yang et al., 2010; Lu et al., 2011; Ren et al., 2016; Tang et al., 2016). Wu et al. (2009) and Sun et al. (2013) found that the vertical dynamic and thermal variations within the ABL influence pollutant concentrations. Quan et al. (2013) compared ABL evolution during clear and haze conditions in Tianjin and considered the possibility of a positive feedback cycle between atmospheric aerosols and lower ABL height, which would induce heavy surface-level pollution in cities. Liu et al. (2015) analyzed ABL characteristics during a typical haze process in January 2014 over the Pearl River Delta region and found that weak wind, low ABL height, and a thermal inversion layer under stable atmospheric conditions were major reasons for haze formation. Based on field measurements similar studies have also been conducted in other megacities or regions, such as the Beijing–Tianjin–Hebei region (Wang et al., 2014; Liao et al., 2014), Xi'an in Western China (Wang et al., 2016), and Eastern China (Li et al., 2015; Peng et al., 2016), but such studies are still very rare in Northeast China (Zhang et al., 2010a, 2010b; Liu et al., 2011). These previous studies have contributed to our understanding of the effects of ABL evolution on the changes in surface air pollution and provide a reference for studies of the interaction of ABL meteorology and aerosols in haze/fog modeling and prediction (Wang et al., 2015a, 2015b).

In this study, the characteristics of ABL structure during a persistent, severe regional haze-fog event over the central Liaoning City Cluster during 16–21 December 2016 were analyzed, using the vertical profiles of ABL meteorological parameters and surface PM concentrations and combined with horizontal wind fields retrieved from the European Centre for Medium Range Weather Forecasts (ECMWF) reanalysis data and back trajectory analyses from the Hybrid Single-Particle Lagrangian Integrated Trajectory (HYSPLIT) model. In Section 2, a brief introduction to the study area and details of the data and methods are described. The results and discussion, given in Section 3, mainly address temporal variation in PM concentrations and the horizontal and vertical structure of the boundary layer. Finally, the conclusions of the study are presented in Section 4.

2. Data and methods

2.1 Description of the study area

Liaoning province is an industrial region that has made a substantial contribution to the economic development of Northeast China (Che et al., 2015). Our study focused on the central Liaoning City Cluster, which comprises Shenyang, Anshan, Fushun, and Benxi (Fig. 1a). These four urban cities are located in a heavily populated industrial region of Northeast China (118.53–125.46°E, 38.43–43.26°N), a major source area for aerosol pollution originating from a variety of human activity, industrial, and transportation sources (Ma et al., 2012; Zhao et al., 2013a; Che et al., 2015). Particularly in winter, emissions from coal burning for domestic heating are a well-established source of pollution (Zhao et al., 2013b; Che et al., 2015).

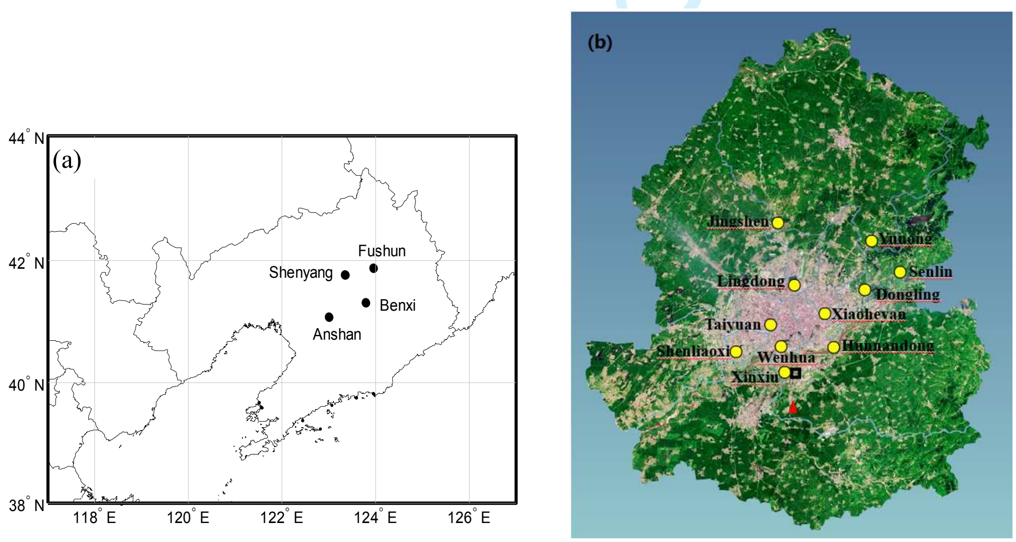

Fig. 1. (a) Geographical locations of the four study cities in the central Liaoning City Cluster of Northeast China, and (b) positions of eleven environmental monitoring

stations (yellow circle), LiDAR (black square), and the boundary layer experiment (red triangle) in Shenyang.

2.2 PM concentrations and surface meteorological parameters

Large-scale regional haze-fog pollution in recent years has been characterized by high concentrations of $PM_{2.5}$ (Wang et al., 2014a). In this study, the hourly mass concentrations of PM_{10} and $PM_{2.5}$ in Shenyang, Anshan, Fushun, and Benxi during a typical haze-fog event during 16–22 December 2016 were obtained from the Liaoning real-time air quality monitoring system (http://211.137.19.74:8089/). There are eleven monitoring stations located in Shenyang, seven in Anshan, and six each in Fushun and Benxi. The ambient real-time particulate monitor is used to measure the concentrations of $PM_{2.5}$ (Model 5030i, Thermo. Sci.) and PM_{10} (Model 5014i, Thermo. Sci.) at each station. The $PM_{2.5}$ and PM_{10} data used in this study were the averages of all the stations in each city and were considered to be representative of the entire city.

The simultaneous hourly mean surface meteorological parameters, i.e., wind speed (U), wind direction (WD), air temperature (T_a), relative humidity (RH), and atmospheric visibility (Vis), from the national weather stations in the four cities were used to identify haze and fog episodes and to analyze the surface meteorological conditions during the haze-fog event.

2.3 Boundary layer structure

The ECMWF reanalysis data, with a spatial resolution of 0.125° × 0.125°, were used to retrieve the horizontal flow fields at 10 m above ground level (AGL) over Liaoning from 16 to 22 December 2016. The ECMWF data were obtained four times a day, at 00:00, 06:00, 12:00, and 18:00 Coordinated Universal Time (UTC), and can be freely downloaded from http://apps.ecmwf.int/datasets/data/interim-full-daily/levtype=sfc/.

To study the vertical structure of the boundary layer during a haze-fog event, a boundary layer observational campaign was conducted from 11:00 LT on 17 December to 14:00 LT on 23 December 2016 in Baitapu Town (123.4160°E, 41.6841°N), about 8 km from the southern edge of the main urban zone of Shenyang (Fig. 1b). The Model CZTK-1 sounding system, developed by the Institute of Atmospheric Physics of the Chinese Academy of Sciences, was used to measure the vertical distributions of U, WD, T_a, and RH, with detective resolution of 0.1 m s^{-1}, 0.1°, 0.1□, and 0.1%, respectively. Sounding balloons were released at an open balcony of a low building (height < 3 m) eight times per day, at 02:00, 05:00, 08:00, 11:00, 14:00, 17:00, 20:00, and 23:00 local time (LT), and a total of 50 groups of profile data were obtained. The ascending velocity of the sounding balloons was about 150 m min^{-1}, and sounding data were recorded at an interval of 1 s. The detection duration was about 20–40 min, and the detection height usually reached up to 1500–4500 m. It should be noted that no precipitation occurred from 17 to 21 December during the haze-fog event but snow weather lasted during 22–23 December 2016 after the haze-fog event. Following the methods used in Liu et al. (2015), vector winds at different observational heights were first calculated based on the vertical profiles of U and WD, and then interpolated at each 50-m AGL. The T_a

and *RH* profiles were averaged every 10 m after data quality control.

2.4 Estimation of boundary layer height

We used two methods to estimate the atmospheric boundary layer height (ABLH). One method used the vertical T_a profiles from sounding data based on the theory of boundary layer evolution (Stull, 1988), with ABLH estimated at the altitude where the temperature was coldest (Wilczak et al., 1996). The other method was based on vertical measurements of the extinction coefficient of aerosols by a ground-based instrument of Light Detection And Ranging (LiDAR) (AGHJ-I-LIDAR), and ABLH was automatically determined at an altitude where a sudden decrease in the scattering coefficient occurred (Cohn and Angevine, 2000; Brooks, 2003). The LiDAR was installed on the roof of the Northeast Regional Meteorological Observation Center (123.4186°E, 41.7344°N) in Shenyang (Fig. 1b); therefore, the building height (60 m) need to be added to the ABLH retrieved by LiDAR. To compare the values of ABHL estimated from the two approaches, the original 1-min LiDAR-measured ABHL were averaged over the first half of every hour.

2.5 Back trajectory analyses

The Hybrid Single-Particle Lagrangian Integrated Trajectory (HYSPLIT) model from the National Oceanic and Atmospheric Administration (NOAA) was used to analyze the transport path of atmospheric pollutants during the haze-fog event (Draxler and Polph, 2003). Two-day back trajectory analyses were conducted for Shenyang (123.50°E, 41.77°N), Anshan (123.00°E, 41.08°N), Fushun (123.95°E, 41.88°N), and Benxi (123.78°E, 41.32°N), and the target altitudes were set at 200, 500, and 1000 m AGL.

3. Results and discussion

3.1 Description of the haze-fog event in the central Liaoning City Cluster

A heavy haze-fog pollution covered the central Liaoning City Cluster during 16–21 December 2016. The air quality in most cities of the central Liaoning City Cluster reached Level 5 (daily air quality index > 200) according to the ambient air quality standards in China. Figure 2 showed the temporal variation of hourly PM concentrations in Shenyang, Anshan, Fushun and Benxi during 16–21 December 2016. In Shenyang the mean PM_{10} and $PM_{2.5}$ concentrations during the haze-fog events were 209.5 and 157.8 μg m^{-3}, respectively, with a mean ratio $PM_{2.5}/PM_{10}$ of 75.3% and with a mean visibility of 1.94 km (Fig. 2a), which is consistent with the results from previous literatures that low visibility is influenced markedly by fine particles in Northeast China (Ma et al., 2011; Zhao et al., 2013a, 2013b). Like in Shenyang, PM in the near-surface atmosphere were accumulating mainly from 19 to 21 December in all cities. The $PM_{2.5}$ concentration during the haze-fog event was larger in Anshan (158.3 ± 22.2 μg m^{-3}) and Shenyang (157.9 ± 31.0 μg m^{-3}) and smaller in Fushun (121.3 ± 48.9 μg m^{-3}) and Benxi (135.6 ± 60.8 μg m^{-3}). It is interesting to find that the first PM peak occurred in Shenyang at first, followed by Anshan, Fushun, and then Benxi, which was likely related to the regional transport of air pollutants.

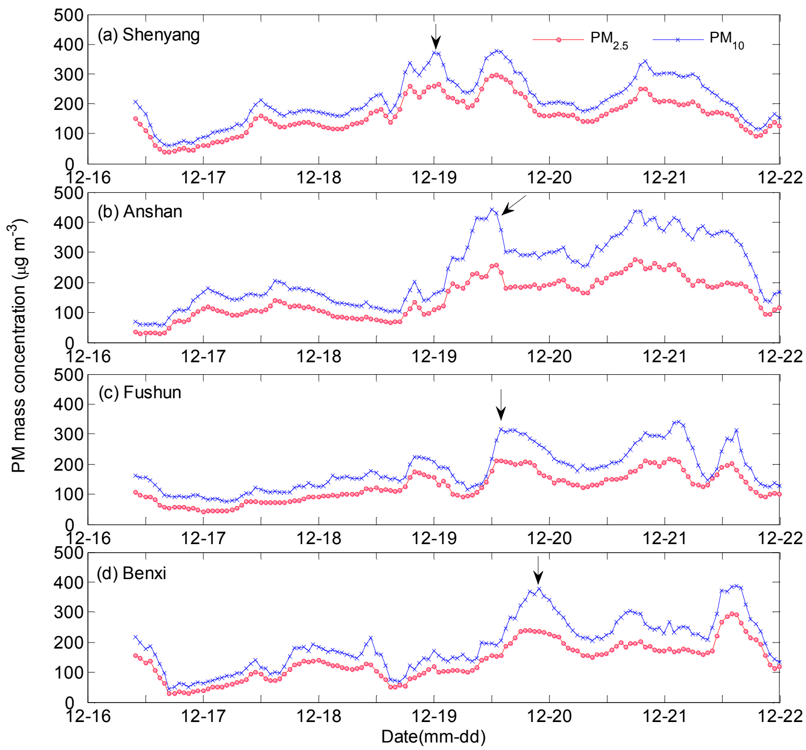

Fig. 2. Temporal variations of hourly mass concentrations of $PM_{2.5}$ and PM_{10} in (a) Shenyang, (b) Anshan, (c) Fushun, and (d) Benxi from 16 to 21 December 2016. The arrows mark out the first PM peaks.

A haze period can be identified by the criteria of *Vis* ≤10 km and *RH* ≤90% (Wu et al., 2007), and same as a fog period, including slight fog characterized by 1 km < *Vis* ≤ 10 km and *RH* >90% and fog characterized by *Vis* ≤1 km and *RH* >90%. The duration of different haze and fog periods as well as the mean and standard deviation of PM concentrations and some surface meteorological parameters are statistically summarized in Table 1. The transformation from haze to fog usually occurred in the afternoon, probably due to the increasing *RH* under cold air conditions after sunset. The *Vis* in fog episodes was lower than that in haze episodes. In Shenyang, the mean

Vis during all fog periods (0.83 km) was 70% lower than that during haze periods (2.77 km). Some previous studies have indicated that an increase in *RH* within a certain range can cause significant *Vis* degradation (Stock et al., 2011; Liu et al., 2012).

Table 1. Statistical summary (mean ± standard deviation) of particulate matter (PM) concentrations and selected surface meteorological parameters during haze and fog periods in the four cities. The letter “H” and “F” represents haze and fog, respectively.

City		Period	PM_{10} (μg m^{-3})	$PM_{2.5}$ (μg m^{-3})	*Vis* (km)	*RH* (%)	*U* (m s^{-1})	T_a (□)
SY	H	12-16 07:00–12-17 15:00	123.2±49.9	86.7±39.4	4.69±2.31	72.6±7.7	1.58±0.80	-3.8±4.4
	F	12-17 16:00–12-18 01:00	171.0±5.8	129.3±6.2	1.28±0.45	94.7±2.0	0.59±0.46	-3.2±1.7
	H	12-18 02:00–12-18 08:00	171.1±12.0	125.9±8.7	1.58±0.61	71.0±10.0	0.44±0.23	4.4±2.3
	F	12-18 09:00–12-19 01:00	273.2±66.5	208.2±45.1	0.62±0.23	96.2±1.6	0.44±0.33	-1.5±2.0
	H	12-19 02:00–12-20 07:00	259.8±64.3	207.2±49.7	1.56±0.54	82.8±5.1	1.21±0.49	1.5±0.7
	F	12-20 08:00–12-21 01:00	265.8±50.4	197.7±31.1	0.59±0.29	96.1±2.3	1.21±0.62	-2.2±0.6
	H	12-21 02:00–12-22 00:00	201.9±63.8	150.4±36.5	3.26±0.98	78.3±3.5	3.80±0.97	-6.0±4.1
AS	H	12-18 10:00–12-18 21:00	132.8±33.1	88.0±22.4	5.68±2.97	78.8±4.3	1.11±0.36	3.6±0.6
	F	12-18 22:00–12-19 01:00	162.8±12.8	111.5±10.5	2.36±0.41	92.0±1.2	1.3±0.20	3.0±0.1
	H	12-19 02:00–12-20 15:00	320.6±51.9	201.9±24.4	4.05±0.97	79.9±5.3	1.26±0.43	1.7±1.2
	F	12-20 16:00–12-21 09:00	389.4±26.2	231.8±31.7	3.74±3.61	91.8±5.5	2.0±0.60	-1.3±0.4
FS	H	12-16 21:00–12-17 11:00	118.3±281.2	76.4±21.9	3.84±2.51	72.8±11.7	1.64±0.59	-1.2±3.6
	F	12-17 12:00–12-19 01:00	184.1±29.9	137.7±23.9	1.11±0.40	93.7±1.0	1.43±0.67	-3.1±1.9
	H	12-19 02:00–12-20 12:00	214.2±61.1	150.4±38.3	1.05±0.37	83.4±7.4	1.18±0.50	1.3±1.4
	F	12-20 13:00–12-21 00:00	269.4±36.6	186.9±23.9	0.97±0.31	91.9±1.2	1.81±0.73	-4.0±0.5
	H	12-21 01:00–12:22 00:00	211.5±75.7	145.2±40.2	2.24±0.87	79.6±3.1	3.57±1.82	-3.6±3.9
BX	H	12-16 18:00–12-17 14:00	128.0±46.0	89.3±35.0	4.20±2.17	75.4±10.5	1.62±0.56	-0.8±4.4
	F	12-17 15:00–12-18 23:00	112.9±35.9	79.1±25.1	1.76±0.16	92.3±1.3	1.84±0.14	-1.5±0.5
	H	12-19 00:00–12-20 16:00	240.8±72.0	170.5±45.2	1.57±0.53	80.1±10.8	1.23±0.46	1.6±2.3
	F	12-20 17:00–12-21 00:00	261.5±24.4	183.4±11.1	1.30±0.39	92.1±1.8	1.40±0.28	-2.8±0.5
	H	12-21 01:00–12:22 00:00	257.6±78.0	193.2±55.2	2.06±0.78	81.7±3.2	1.91±0.63	-4.7±4.4

3.2 Effects of boundary layer structure on the haze-fog event

3.2.1 Characteristics of horizontal wind fields

Vector wind field reflects the regional flow spatial characteristics; a larger vector wind indicates better dispersion conditions for air pollutants, and vice versa (Wu et al., 2008). Figure 3 depicts the average daily 10-m wind fields during 16–21 December 2016 over Liaoning. Southwesterly and westerly flows dominated in Liaoning on 16 December, and U was the largest in the coastal area of the Bohai Sea. A belt of high-value U covered the Liaoning central area, extending from the southwest to the northeast. Shenyang and Anshan were located at the east side of the belt of high U, and Fushun and Benxi were located on the edge of an area of low U in the eastern region of Liaoning (Fig. 3a). On 17 December, the southwesterly flow turned to a southeasterly flow over the Liaoning central area, and U decreased over large parts of Liaoning, except the eastern region (Fig. 3b). The southerly flows favored the transport of water vapor from the Bohai Sea to Liaoning. Wind speed continually decreased during 18–20 December (Fig. 3c–e), and a belt of low U formed along the Anshan–Benxi line on 20 December (Fig. 3e), which was favorable for the accumulation of air pollutants in this region. With the arrival of cold and dry air masses brought by the strong northeasterly flows on 21 December, the heavy haze-fog event ultimately ended (Fig. 3f).

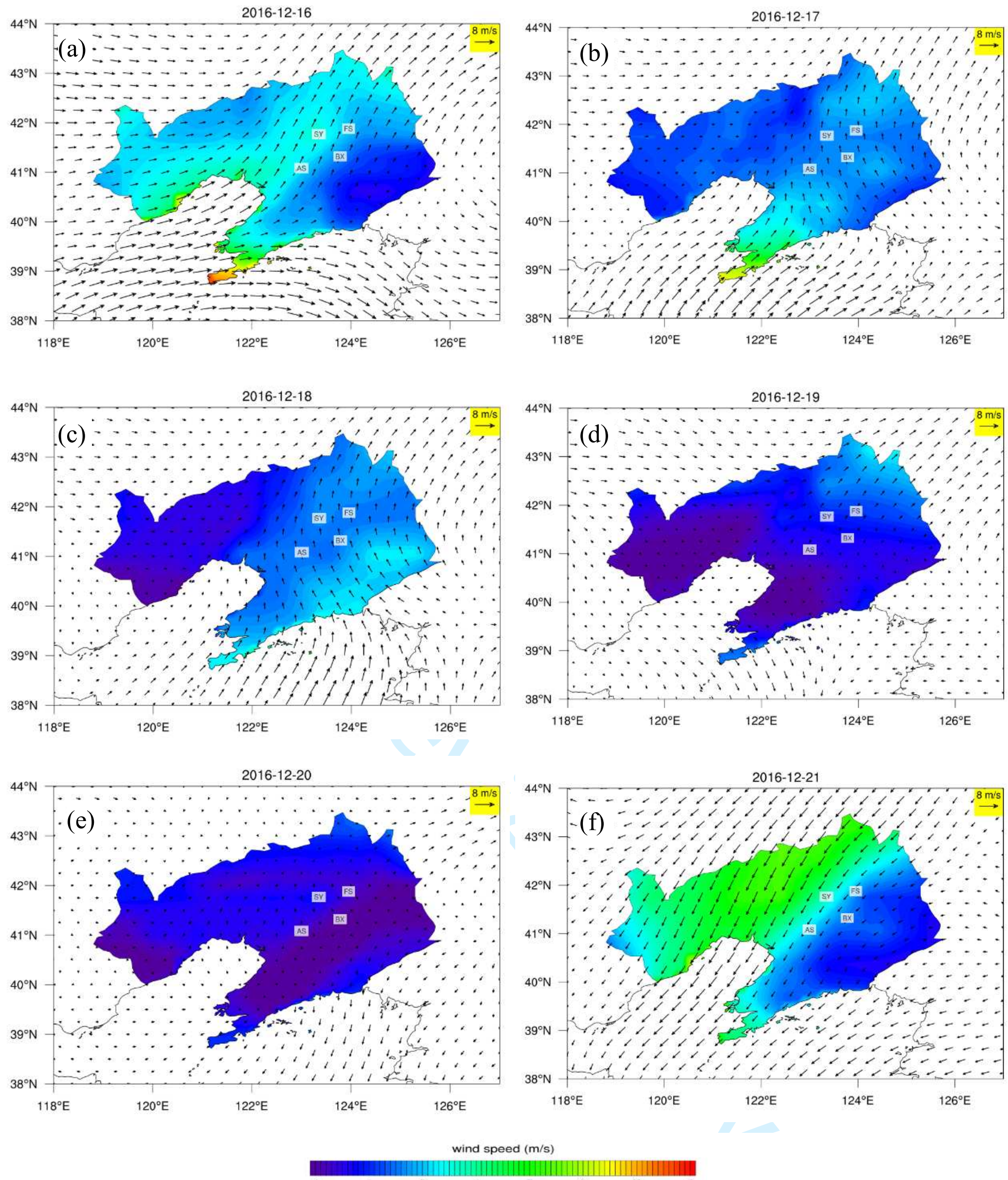

Fig. 3. Spatial variations of the daily mean wind field over Liaoning province from 16 to 21 December 2016.

3.2.2 Characteristics of the vertical wind distribution

The vertical distribution of vector wind derived from sounding data during the haze-fog event in Shenyang is shown in Fig. 4. The haze-fog event could be divided into five different periods, according to the wind shear characteristics. During Period

1 (11:00 LT on 17 December to 08:00 LT on 18 December), the *WD* rotated with increasing height in a clockwise direction, varying from the southeast to the southwest, and the *WD* shear height reduced gradually from 600 m to 200 m with time, which was probably related to the strengthening downdraft (Liu et al., 2015). Meanwhile, there exists a strong wind shear in the lower layer (<600 m), and *U* increased rapidly with increasing height. During Period 2 (11:00 LT on 18 December to 11:00 LT on 19 December), stable southerly and southwesterly flows prevailed within the ABL in Shenyang, and *U* at all heights was very low, especially at low altitudes, which favored the accumulation of air pollutants (Fig. 2a). Period 3 (14:00 LT on 19 December to 05:00 LT on 20 December) was characterized by frequent changes in *WD* and persistently weak *U*. During Period 4, *U* remained low at low altitudes, whereas at high altitudes (>700 m), *U* initially increased and then declined sharply again. After 14:00 LT on 21 December, in Period 5, *U* at middle altitudes began to increase, and a change in *WD* occurred at low altitudes. Combined with the evolution of the PM concentration shown in Fig. 2a, weak *U* and wind shear within the ABL hindered the vertical dispersion of pollutants, whereas with the arrival of cold air, the dynamic stability of the ABL collapsed, leading to a rapid reduction in the surface PM concentration.

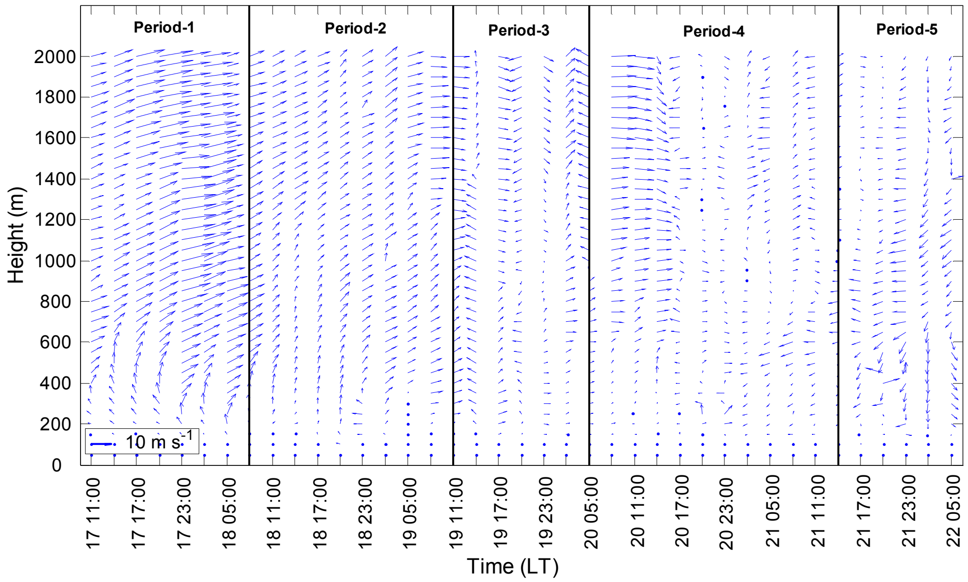

Fig. 4. Vertical distribution of vector wind in Shenyang from 11:00 on 17 December to 05:00 on 22 December 2016.

3.2.3 Characteristics of vertical temperature distributions

The vertical distribution of T_a during the haze-fog event in Shenyang is shown in Fig. 5. Convective mixing layer between the surface and 1000 m AGL developed during the early haze-fog period before 19 December, but the depth of the warm layer declined due to cold air that descended over time from high to low altitudes, resulting in a strong and deep thermal inversion layer above the ground on 20 December. These stable and upper-layer warm atmospheric conditions were very favorable for the maintenance of the haze-fog pollution event.

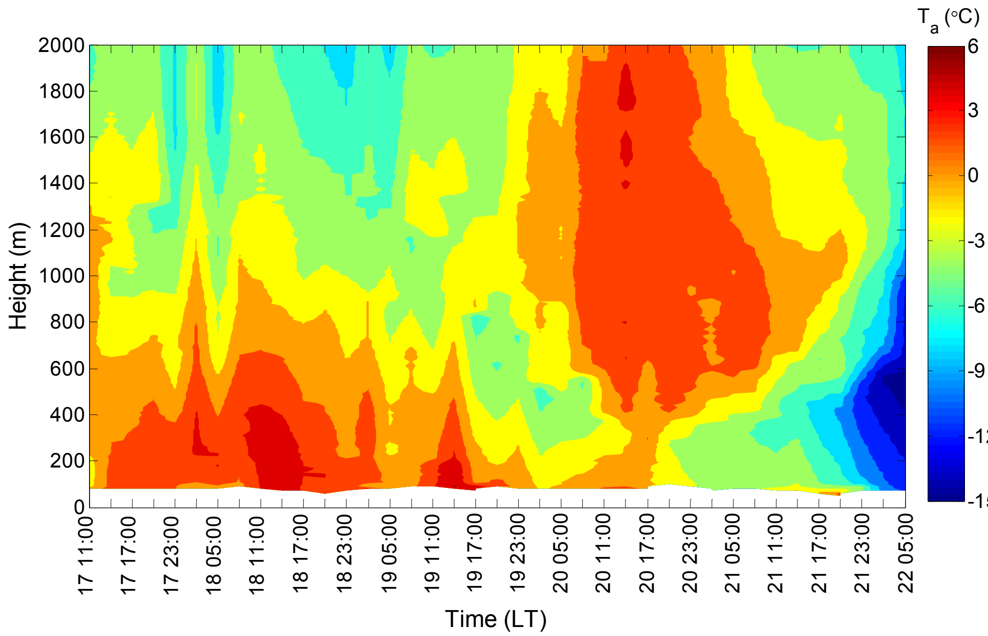

Fig. 5. Vertical distribution of air temperature in Shenyang from 11:00 on 17 December to 05:00 on 22 December 2016.

To clearly outline the evolution of the vertical distribution of T_a, Fig. 6 shows temperature profiles in Shenyang at 11:00 and 23:00 LT from 17 to 22 December 2016. Two weak inversion layers occurred at 11:00 LT on 17 December. One occurred at 170–350 m AGL, with an inversion intensity of 2.6 □/km, and the other occurred at 770–910 m AGL, with an intensity of 1.3 □/km. However, the two inversion layers disappeared at 23:00 LT on 17 December, and a new ground inversion layer formed (Fig. 6a). During 18 and 19 December (Fig. 6b, 6c) there was little variation of T_a with height, and many thermal inversion layers existed within the ABL. A strong inversion layer then formed and was maintained in the near-surface layer; the bottom of this inversion layer varied from 200 to 350 m during 11:00 LT on 20 December to 11:00 LT on 21 December (Fig. 6d, 6e). Such stable atmospheric stratification at low altitudes was very helpful for the accumulation of PM concentrations. Due to the invasion of cold air at low altitudes, the bottom of this inversion layer was lifted up to 900 m at 11:00 LT, and the inversion layer disappeared at 23:00 LT on 22 December (Fig. 6f), which strengthened the vertical mixing of air pollutants.

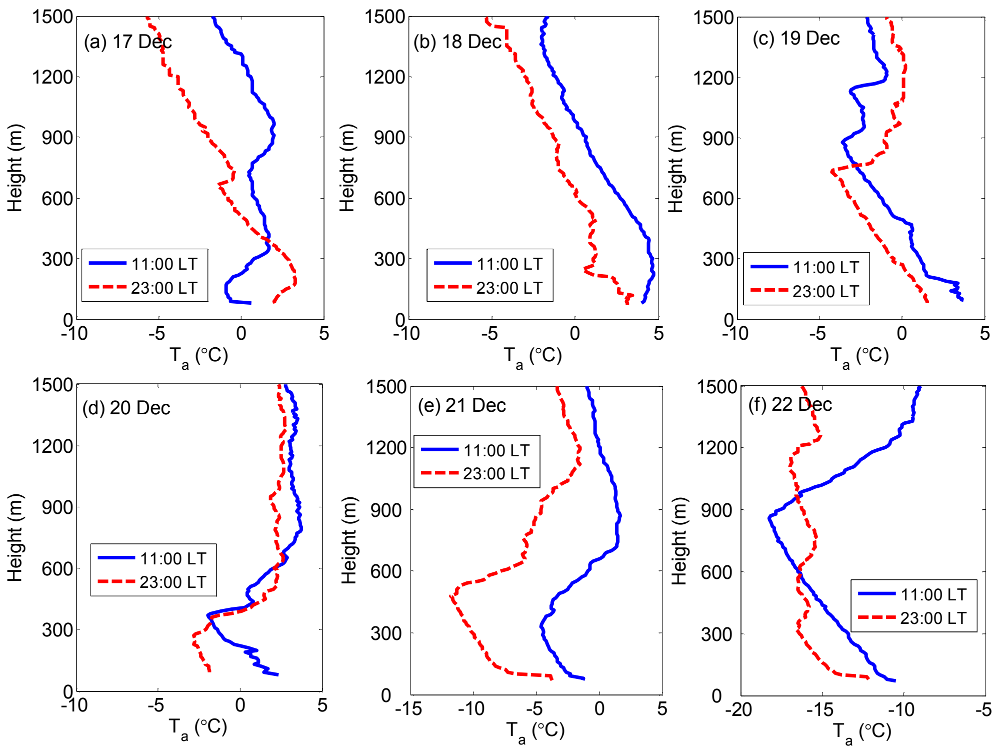

Fig. 6. Temperature profiles for Shenyang at 11:00 LT and 23:00 LT on (a) 17, (b) 18, (c) 19, (d) 20, (e) 21, and (f) 22 December 2016.

3.2.4 Evolution of ABHL

The ABLH plays an important role in the evolution of haze-fog episodes. The ABLH values measured by LiDAR and those estimated using sounding data displayed similar variation (Fig. 7), and both had a negative correlation with the PM concentration, with correlation coefficient R = -0.36 for LiDAR and R = -0.21 for sounding data, respectively. The regular diurnal variation of ABLH, i.e., highest in the middle of the day and lowest at nighttime, was not observed during the haze-fog event. The ABLH measured by LiDAR was <700 m during the haze-fog event, with the lowest value being 100 m at 02:00 LT on 21 December, and then gradually increased to 800 m as the haze-fog event ended. The ABLH measured by balloon sounding was higher than that determined by LiDAR, particularly when the ABLH was high, which corresponded to low PM concentrations. The ABLH measured by ball sounding is typically below 400 m during heavy pollution episodes. Such low ABLH levels led to high PM concentration in the near-surface layer. It turned out that the ABLH determined by LiDAR was comparable to that estimated using sounding data in Shenyang, and the LiDAR measurements can be used to obtain real-time ABLH for further study.

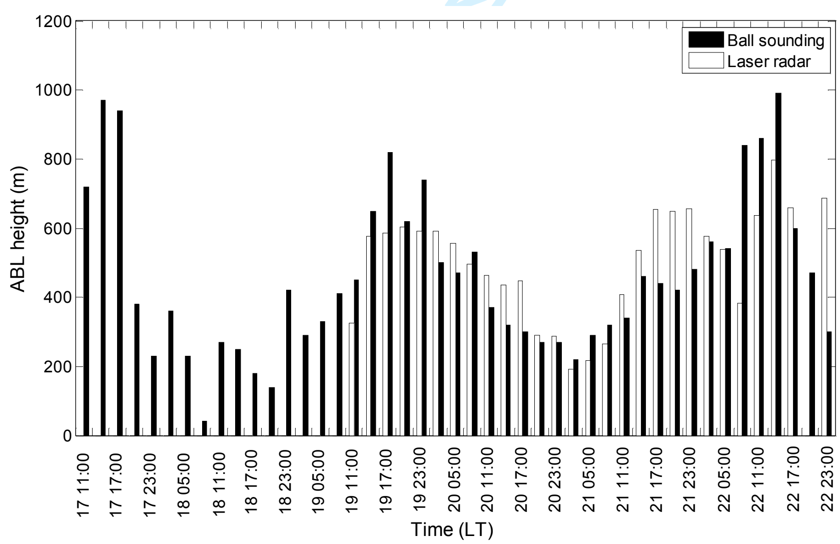

Fig. 7. Evolution of atmospheric boundary layer height (ABLH) measured by ball sounding and LiDAR in Shenyang.

3.3 Back trajectory results

Different aerosol transportation paths were observed in the four cities during the haze-fog event according to the 2-day back trajectory analyses at 200, 500, and 1000 m AGL (Fig. 8), which ended with the occurrence of the first PM concentration peak in Fig. 2. The air masses at 200 m AGL were generated from the Bohai Sea and passed through North Korea and southeastern Liaoning before arriving at Shenyang, Fushun, and Benxi. These air masses carried water vapor and led to high *RH* conditions. However, the air masses at all three altitudes in Anshan originated from western China (Fig. 8b), resulting in lower *RH* in Anshan than in the other three cities. The transportation paths of air masses at 1000 m AGL in Fushun and Benxi were similar to that of the air mass that arrived in Anshan. The air masses at the middle altitude of 500 m AGL in Shenyang originated from the North China Plain, where anthropogenic activities are intense and severe haze pollution is common. This might explain why the haze-fog event first occurred in Shenyang.

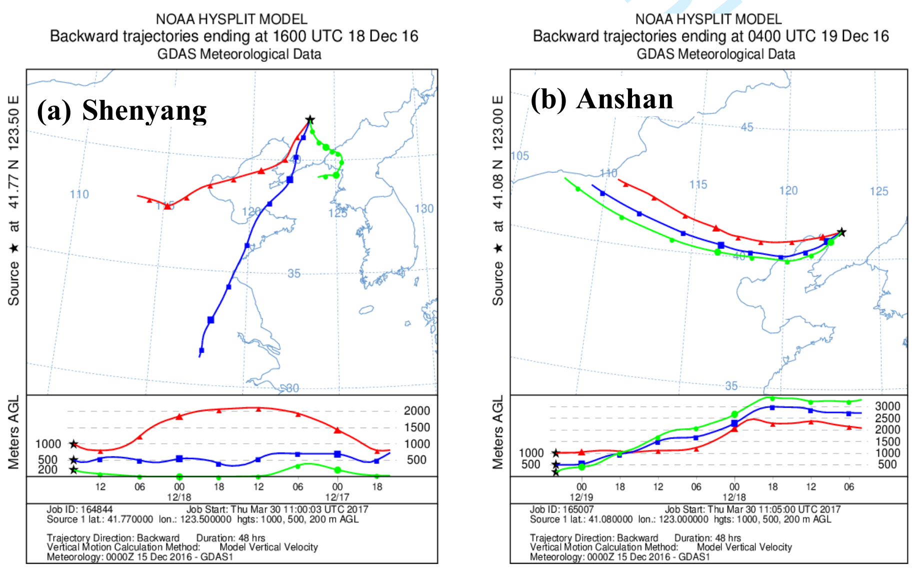

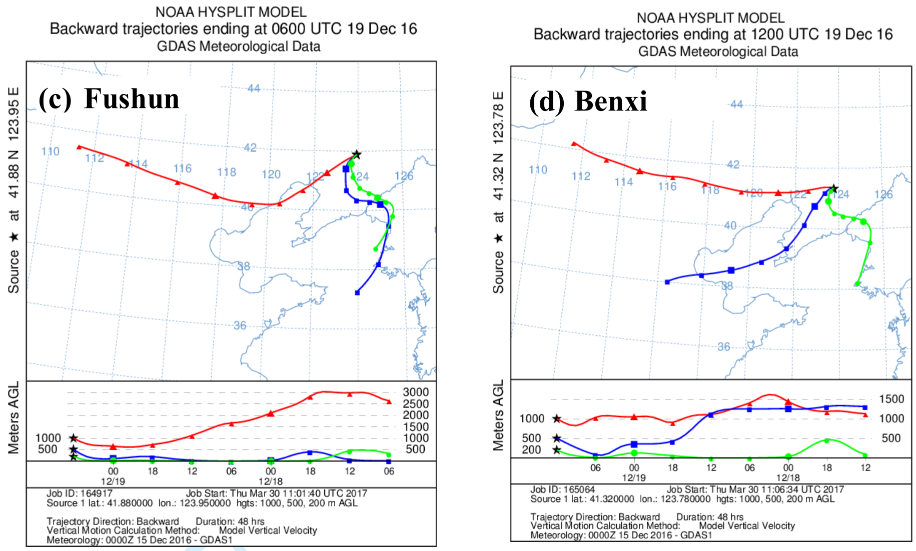

Fig. 8. The 48-h backward trajectory in (a) Shenyang, (b) Anshan, (c) Fushun, and (d) Benxi starting from the first peak of the PM concentration during the haze-fog event.

4. Conclusion

The characteristics of the ABL structure during a persistent, severe regional haze-fog event over the central Liaoning City Cluster during 16–21 December 2016 were analyzed based largely on measurements from an ABL observational experiment and PM concentrations at the surface. The haze-fog pollution began in Shenyang at first, at 12:00 LT on 16 December, and ended at about 00:00 LT on 21 December in all four cities. The $PM_{2.5}$ concentration during the haze-fog event was larger in Anshan (158.3 ± 22.2 μg m^{-3}) and Shenyang (157.9 ± 31.0 μg m^{-3}) and smaller in Fushun (121.3 ± 48.9 μg m^{-3}) and Benxi (135.6 ± 60.8 μg m^{-3}). According to the variations of *RH* and *Vis*, several haze and fog episodes were distinguished. The transformation from haze to fog usually occurred in the afternoon, which is probably related to the increasing *RH* under cold air conditions after sunset.

The distribution of daily horizontal wind fields at 10 m AGL that were retrieved from the ECMWF reanalysis data during 16–21 December were strongly related to allocation of the surface pressure field. Southwesterly and westerly flows dominated in Liaoning on 16 December, and a belt of high *U* covered the Liaoning central area, extending from the southwest to northeast. On 17 December, the *U* veered into the southeast over the Liaoning central area, and *U* decreased persistently during 18–20 December, which was favorable for the accumulation of air pollutants and water vapor in this region. With the arrival of cold and dry air masses carried by the strong northeasterly flows on 21 December, the heavy persistent haze-fog event ultimately ended.

According to the analyses of the vertical distribution of temperature, a thick warm layer between the surface and 1000 m AGL developed during the early haze-fog period before 19 December, but the top of the warm layer declined due to cold air that descended over time from high to low altitudes. This resulted in a strong and deep thermal inversion layer, with the bottom lying at 200–350 m AGL in the near-ground layer on 20 December. These stable and warm atmospheric conditions were very favorable for the formation and maintenance of the haze-fog pollution event. The ABLH measured by ball sounding is typically less than 400 m during a heavy pollution episode. Such a low ABLH would concentrate pollutants in the near-surface layer. The stable atmospheric stratification finally acted on the vertical distribution of the wind field in the boundary layer, further weakening the exchange capacity of the vertical turbulence. The superposition of a weak wind field with weak horizontal wind resulted in air stagnation, ultimately causing deterioration in air quality during the haze-fog event.

The back trajectory analyses indicated that the air masses at the lower altitude of 200 m AGL in all cities originated from North Korea and passed over the Bohai Sea, except for the air masses arriving in Anshan, which caused lower humidity there compared with that in the other cities. The air masses at the higher altitudes of 500 and 1000 m AGL in Shenyang were generated from the North China Plain, where anthropogenic activities are intense and haze pollution is severe. The air masses arriving in the other cities originated from western China or over the Bohai Sea, which might explain why the haze-fog event occurred firstly in Shenyang.

Reference

Brooks, I. M., 2003: Finding boundary layer top: Application of a wavelet covariance transform to lidar backscatter profiles. *J. Atmos. Oceanic Technol.*, **20**, 1092–1105.

Chan, C.K., and X.H. Yao, 2008: Air pollution in megacities in China. *Atmos. Environ.*, **42(1)**, 1–42.

Che, H., X. Xia, J. Zhu, et al., 2014: Column aerosol optical properties and aerosol radiative forcing during a serious haze-fog month over North China Plain in 2013 based on ground-based sunphotometer measurements. *Atmos. Chem. Phys.*, **14(4)**, 2125–2138.

Che, H., H. Zhao, X. Xia, et al., 2015: Fine Mode Aerosol Optical Properties Related to Cloud and Fog Processing over a Cluster of Cities in Northeast China. *Aerosol Air Qual. Res.*, **15(5)**, 2065–2081.

Chen, J., C. S. Zhao, N. Ma, et al, 2012: A parameterization of low visibilities for hazy days in the North China Plain. *Atmos. Chem. Phys.*, **12(11)**, 4935–4950.

Chen, W.W., D.Q. Tong, M. Dan, et al., 2016: Typical atmospheric haze during crop harvest season in northeastern China: A case in the Changchun region. *J. Environ. Sci.*, in press.

Chen, Z. H., S. Y. Cheng, J. B. Li, et al., 2008: Relationship between atmospheric pollution processes and synoptic pressure patterns in northern China. *Atmos. Environ.*, **42(24)**, 6078–6087.

Cohn, S. A., and W. M. Angevine, 2000: Boundary layer height and entrainment zone thickness measured by lidars and wind-profiling radars. *J. Appl. Meteor.*, **39**, 1233–1247.

Cui Yan, Zhao Chunyu, Wang Tao, et al., 2015: Temporal and spatial characteristics of haze days with different intensities and the climatic factors during 1961–2013 in Liaoning Province. *Acta Scientiae Circumstantiae*, **35(6)**, 1629–1637. (in Chinese)

Draxler, R.R., and G.D. Rolph, 2003: Hybrid Single-Particle Lagrangian Integrated Trajectory Model access via NOAA ARL READY. NOAA Air Resources Laboratory, Silver Spring, MD. Website: http://www.ready.noaa.gov/HYSPLIT.php

Fu, G. Q., W. Y. Xu, R. F. Yang, et al., 2014: The distribution and trends of fog and haze in the North China Plain over the past 30 years. *Atmos. Chem. Phys.*, **14(21)**, 11949–11958.

Ji, D., Y. Wang, L. Wang, et al, 2012: Analysis of heavy pollution episodes in selected cities of northern China. *Atmos. Environ.*, **50**, 338–348.

Li Minna, Niu Shengjie, Zhang Shuting, et al., 2015: Comparative study of turbulent characteristics between the fog day and haze day in Nainjing. *Acta meteorological Sinica*, **73(3)**, 593–608. (in Chinese)

Liao Xiaonong, Zhang Xiaoling, Wang Yingchun, et al., 2014: Comparative analysis on meteorological condition for persistent haze cases in summer and winter in Beijing. *Environ. Sci.*, **35(6)**, 2031–2044. (in Chinese)

Liu Jian, Fan Shaojia, Wu Dui, et al., 2015: Boundary layer characteristics of typical haze process in the Pearl River Delta region. *China Environ. Sci.*, **35(6)**, 1664–1674. (in Chinese)

Liu, S.H., Z.X. Liu, J. Li, et al., 2009: Numerical simulation for the coupling effect of local atmospheric circulations over the area of Beijing, Tianjin and Hebei province. *Sci. China Ser. D Earth Sci.*, **52(3)**, 382–392

Liu, X.G., Y.H. Zhang, Y.F. Cheng, et al., 2012: Aerosol hygroscopicity and its impact on atmospheric visibility and radiative forcing in Guangzhou during the 2006 PRIDE-PRD campaign. *Atmos. Environ.*, **60**, 59–67.

Liu Ningwei, Ma Yanjun, Liu Xiaomei et al., 2011: Observations on haze and fog in Shenyang area. *Acta Scientiae Circumstantiae*, **31(5)**, 1064–1069. (in Chinese)

Lu Chunsong, Niu Shengjie, Yueping, et al., 2011: Observational research on boundary layer structure during high incidence period of winter fog in Nanjing. *Trans. Atmos. Sci.*, **34(1)**, 58–65. (in Chinese)

Ma Yanjun, Liu, Ningwei, Wang Yangfeng, et al., 2011: The distribution characteristics of fine particles and their impact on air quality in Shenyang and surrounding areas. *Acta Sci. Circum.*, **31**, 1168–1174. (in Chinese)

Ma Yanjun, Liu Ningwei, Hong Ye, et al., 2012: The impacts on various particles sizes and the quality caused by a dust weather process in spring 2011 in Liaoning. *Acta Sci. Circum.*, **32**, 1160–1167 (in Chinese).

Miao, Y., S. Liu, Y. Zheng, et al., 2015: Numerical study of the effects of local atmospheric circulations on a pollution event over Beijing–Tianjin–Hebei, China. *J. Environ. Sci.*, **30**, 9–20.

Peng, H., D. Liu, B. Zhou, et al., 2016: Boundary-layer characteristics of persistent regional haze events and heavy haze days in Eastern China. *Adv. Meteor.*, **6950154**. http://dx.doi.org/10.1155/2016/6950154.

Quan, J., Y. Gao, Q. Zhang, et al., 2013: Evolution of planetary boundary layer under different weather conditions, and its impact on aerosol concentrations. *Particuology*, **11(1)**, 34–40.

Shao, M., X. Tang, Y. Zhang, et al., 2006: City clusters in China: air and surface water pollution. *Frontiers in Ecology and the Environment*, **4(7)**, 353–361.

Shen, X. J., J. Y. Sun, X. Y. Zhang, et al, 2015: Characterization of submicron aerosols and effect on visibility during a severe haze-fog episode in Yangtze River Delta, China. *Atmos. Environ.*, **120**, 307–316.

Stock, M., Y.F. Cheng, W. Birmili, et al., 2011: Hygroscopic properties of atmospheric aerosol particles over the eastern Mediterranean: implications for regional direct radiative forcing under clean and polluted conditions. *Atmos. Chem. Phys.*, **11(9)**, 4251–4271.

Stull, R. B., 1988. An Introduction to Boundary Layer Meteorology. Kluwer Academic Publishers, Dordrecht.

Sun, Y., T. Song, G. Tang, et al., 2013: The vertical distribution of $PM_{2.5}$ and boundary-layer structure during summer haze in Beijing. *Atmos. Environ.*, **74**, 413–421.

Tang G., P. Zhao, Y. Wang, et al., 2017: Mortality and air pollution in Beijing: The long-term relationship. *Atmos. Environ.*, **150**, 238–243.

Tang, G., J. Zhang, X. Zhu, et al., 2016: Mixing layer height and its implications for air pollution over Beijing, China. *Atmos. Chem. Phys.*, **16**, 2459–2475.

Wang Kai, Zhang Hongsheng, Wang Qiang, et al., 2006: Study on the structure and evolvement of atmospheric boundary layer of frontal fogs in spring and winter at southern suburb of Beijing. *Acta Scientiarum Naturalium Univesitatis Pekinensis*, **42(1)**: 55–60. (in Chinese)

Wang, L., N. Zhang, Z. Liu, et al., 2014a: The influence of climate factors, meteorological conditions, and boundary-layer structure on severe haze pollution in the Beijing-Tianjin-Hebei region during January 2013. *Adv. Meteor.*, **685971**. http://dx.doi.org/10.1155/2014/685971.

Wang, Y.S., L. Yao, L. L. Wang, et al, 2014b: Mechanism for the formation of the

January 2013 heavy haze pollution episode over central and eastern China. *Sci. China Earth Sci.*, **57**, 14–25.

Wang, H., M. Xue, X.Y. Zhang, et al., 2015a: Mesoscale modeling study of the interactions between aerosols and PBL meteorology during a haze episode in Jing–Jin–Ji (China) and its nearby surrounding region–Part 1: Aerosol distributions and meteorological features. *Atmos. Chem. Phys.*, **15(6)**, 3257–3275.

Wang, H., G. Y. Shi, X. Y. Zhang, et al., 2015b: Mesoscale modelling study of the interactions between aerosols and PBL meteorology during a haze episode in China Jing–Jin–Ji and its near surrounding region–Part 2: Aerosols' radiative feedback effects. *Atmos. Chem. Phys.*, **15(6)**, 3277–3287.

Wang, Y. Q., X. Y. Zhang, J. Y. Sun, et al., 2015c: Spatial and temporal variations of the concentrations of PM_{10}, $PM_{2.5}$ and PM_1 in China. *Atmos. Chem. Phys.*, **15(23)**, 13585–13598.

Wang S., T. Liao, L. Wang, et al., 2016: Process analysis of characteristics of the boundary layer during a heavy haze pollution episode in an inland megacity, China. J. *Environ. Sci.*, **40**, 138–144.

Wilczak, J. M., E. E. Gossard, W. D. Neff, et al., 1996: Ground-based remote sensing of the atmospheric boundary layer: 25 years of progress. In J. R. Garratt, & P. A. Taylor (Eds.), Boundary-Layer Meteorology. Kluwer Academic Publishers 25th Anniversary.

Wu Dui, Liao Guolian, Deng Xuejiao, et al, 2008: Transport condition of surface layer under haze weather over the Pearl River Delta. *J. Appl. Meteorl. Sci.*, **19(1)**, 1–9. (in Chinese)

Wu, D., X. Bi, X. Deng, et al., 2007: Effects of atmospheric haze on the deterioration of visibility over the Pearl River Delta. *Acta. Meteorol. Sin.*, **21(2)**, 510–517, 2006.

Wu Zhenling, Liu Aixia, Zhang Changchun, et al., 2009: Vertical Distribution Feature of $PM_{2.5}$ and Effect of Boundary Layer in Tianjin. *Urban Environment & Urban Ecology*, **22(4)**, 24–29. (In Chinese)

Yang Jun, Wang Lei, Liu Ruiyang, et al., 2010: The boundary layer structure and the evolution mechanisms of a deep dense fog event. *Acta Meteorological Sinica*, **68(6)**, 998–1006. (in Chinese)

Zhang, R.H., Q. Li, and R.N. Zhang, 2014: Meteorological conditions for the persistent severe fog and haze event over eastern China in January 2013. *Sci. China Earth Sci.*, **57(1)**, 26–35.

Zhang Yunhai, Ma Yanjun, Liu Ningwei, et al., 2010a: Study on environmental characteristics of haze in Shenyang. *Ecology and Environmental Science*, **19(11)**, 2636–2641. (in Chinese)

Zhang, Y. H., H. B. Yang, X. D. Zou, 2010b: Test research on the characteristics of pollution boundary layer in the river outlet area of Grand Liao River. Meteor. Environ. Res., 1(6): 57–61.

Zhao, H.J., H.Z. Che, X.Y. Zhang, et al., 2013a: Aerosol Optical Properties over Urban and Industrial Region of Northeast China by Using Ground-based

Sunphotometer Measurement. *Atmos. Environ.*, **75**, 270–278.

Zhao, H.J., H.Z. Che, X.Y. Zhang, et al., 2013b: Characteristics of Visibility and Particulate Matter (PM) in an Urban Area of Northeast China. *Atmos. Pollut. Res.*, **4**, 427–434.

Zheng, G. J., F. K. Duan, H. Su, et al, 2015: Exploring the severe winter haze in Beijing: the impact of synoptic weather, regional transport and heterogeneous reactions. *Atmos. Chem. Phys.*, **15(6)**, 2969–2983.

Zhu, J., H. Liao, and J. Li, 2012: Increases in aerosol concentrations over eastern China due to the decadal-scale weakening of the East Asian summer monsoon. *Geophys. Res. Lett.*, **39(9)**, L09809.